Proc. Natl. Acad. Sci. USA
Vol. 96, pp. 9915–9919, August 1999
Neurobiology

Loss of the ataxia–telangiectasia gene product causes oxidative damage in target organs

CARROLEE BARLOW*†‡, PHYLLIS A. DENNERY§, MARK K. SHIGENAGA¶, MARK A. SMITH‖, JASON D. MORROW**, L. JACKSON ROBERTS, II**, ANTHONY WYNSHAW-BORIS*††, AND RODNEY L. LEVINE§§

*Laboratory of Genetic Disease Research, National Human Genome Research Institute, Bethesda, MD 20892; †The Salk Institute for Biological Studies, The Laboratory of Genetics, 10010 North Torrey Pines Road, La Jolla, CA 92037; §Department of Pediatrics, Stanford University School of Medicine, Stanford, CA 94035; ¶Division of Biochemistry and Molecular Biology, 401 Barker Hall, University of California, Berkeley, CA 94720; ‖Institute of Pathology, Case Western Reserve University, Cleveland, OH 44106; **Division of Clinical Pharmacology, Vanderbilt University School of Medicine, Nashville, TN 37232; and §§Laboratory of Biochemistry, National Heart, Lung, and Blood Institute, Bethesda, MD 20892

Edited by E. R. Stadtman, National Institutes of Health, Bethesda, MD, and approved June 25, 1999 (received for review June 1, 1999)

ABSTRACT **Ataxia–telangiectasia (A-T) is characterized by a markedly increased sensitivity to ionizing radiation, increased incidence of cancer, and neurodegeneration, especially of the cerebellar Purkinje cells. Ionizing radiation oxidizes macromolecules and causes tissue damage through the generation of reactive oxygen species (ROS). We therefore hypothesized that A-T is due to oxidative damage resulting from loss of function of the A-T gene product. To assess this hypothesis, we employed an animal model of A-T, the mouse with a disrupted *Atm* gene. We show that organs which develop pathologic changes in the *Atm*-deficient mice are targets of oxidative damage, and that cerebellar Purkinje cells are particularly affected. These observations provide a mechanistic basis for the A-T phenotype and lay a rational foundation for therapeutic intervention.**

Ataxia–telangiectasia (A-T) is an inherited disease causing progressive neurological dysfunction, especially in the cerebellum (1). All known cases are caused by mutations in the *ATM* (for ataxia–telangiectasia-mutated) gene (2), which encodes a protein similar to the phosphatidylinositol 3-kinase (PI 3-kinase) family of kinases (2). A hallmark of patients with A-T, cultured cells from these patients, and *Atm*-deficient mice is markedly increased sensitivity to ionizing radiation (1, 3–5). Ionizing radiation damages macromolecules and kills cells through the generation of reactive oxygen species, suggesting that loss of ATM leads to oxidative damage and disease in A-T. This hypothesis has not yet been rigorously investigated in A-T, but there is substantial evidence implicating oxidative damage in the pathogenesis or progression of other neurodegenerative diseases, including Parkinson's and Alzheimer's diseases (6–8). We previously created an animal model of A-T by disrupting the mouse homologue of *ATM*, referred to as *Atm* (1). The *Atm*-deficient mouse was shown to have many of the characteristics of the human disease, most notably the increased sensitivity to ionizing radiation. The *Atm*-deficient mouse has abnormalities in neuromotor function and spermatogenesis, and has a high incidence of tumors of the thymus. We now show that loss of *Atm* causes oxidative damage in tissues, particularly the Purkinje cells of the cerebellum.

MATERIALS AND METHODS

***Atm*-Deficient Mice.** *Atm*-deficient mice were generated as described (1). Animals used in this study were either inbred 129SvEv or mixed Black Swiss/129SvEv backgrounds. We used animals between 2 and 8 months of age. Because *Atm*-deficient mice often develop aggressive thymic lymphomas beginning at 2 months of age, the thymus of all animals was dissected and examined grossly and microscopically to ensure there were neither gross tumors nor isolated foci of tumors. Animals with any evidence of tumors were not used. All animal procedures were performed according to protocols approved by both The Salk Institute for Biological Studies and the National Institutes of Health Animal Care and Use Committee. Animals were anesthetized with an intraperitoneal avertin injection (80 μg/g of body weight) and either exsanguinated by decapitation or perfused with cold saline. For perfusions the rib cage was reflected to expose the heart, the lower left ventricle was cannulated, and saline solution was infused for 1–2 min to remove blood from the brain. The right atrium was cut to allow outflow of the blood and saline solution. Tissues were collected and flash frozen in liquid nitrogen and stored on dry ice or at −80°C until used in assays or mounted in cryopreservative for frozen sections.

Assays for Markers of Oxidative Damage. Nitrotyrosine assays were performed according to published protocols (9). Briefly, brain and liver tissues were homogenized with 8 passes of a Potter–Elvehjem tissue grinder at 800 rpm in >10 vol of 0.1 M sodium acetate, pH 7.2, supplemented with 0.1 mM desferoxamine mesylate (Sigma). The brain homogenate (0.75 ml) was delipidated by an extraction with methanol/water/chloroform. Liver extracts were not delipidated. Samples were then processed and analyzed for protein-bound 3-nitrotyrosine as the *N*-acetyl-3-aminotyrosine derivative by high-performance liquid chromatography with electrochemical detection.

Protein carbonyl levels were measured by both the quantitative HPLC method and by Western blotting of tissue homogenates from three animals of each genotype (10).

Isoprostane assays were performed on brain, testes, and thymus, which were dissected and flash frozen. F_2-isoprostanes were measured as described (11).

Heme Oxygenase (HO). Northern blots were prepared from 3-month-old male control and *Atm*-deficient mice. Brains were promptly dissected, cortex was separated from cerebellum, and each was flash frozen. RNA was prepared with Trizol reagent, and 10 μg of total RNA was used for preparing Northern blots. The blot was hybridized sequentially with a full-length cDNA probes for HO-1, HO-2, and cyclophilin as a control for RNA loading. The blots were scanned and quantitated with a PhosphorImager (Molecular Dynamics). Tissues were analyzed for HO activity by gas chromatography, in subdued lighting as described (12).

The publication costs of this article were defrayed in part by page charge payment. This article must therefore be hereby marked "*advertisement*" in accordance with 18 U.S.C. §1734 solely to indicate this fact.

PNAS is available online at www.pnas.org.

This paper was submitted directly (Track II) to the *Proceedings* office.
Abbreviations: A-T, ataxia–telangiectasia; ATM, A-T-mutated; PI 3-kinase, phosphatidylinositol 3-kinase; HO, heme oxygenase.
‡To whom reprint requests should be addressed at the † address. E-mail: barlow@salk.edu.
††Present address: Departments of Pediatrics and Medicine, University of California, San Diego School of Medicine, La Jolla, CA 92093.

HO-1 and HO-2 were detected by immunohistochemistry on tissues from mice perfused with phosphate-buffered saline, pH 7.4 (PBS), containing 4% fresh paraformaldehyde. Tissues were sectioned after paraffin embedding, deparaffinized, and permeabilized with 0.3% saponin in PBS and blocked in PBS containing 5% nonfat powdered milk, 1% BSA, and 0.03% saponin. The slides were then incubated with a 1:25 dilution of rabbit anti-rat HO antiserum overnight in a humidified chamber. Polyclonal rabbit anti-rat HO-1 antibodies were raised against a 30-kDa soluble HO-1 protein expressed in *Escherichia coli* from rat liver cDNA (gift of Angela Wilks, University of California, San Francisco). Rabbit anti-rat HO-2 antibodies were obtained from Chemicon (Temecula, CA).

Slides were washed twice in PBS containing 0.03% saponin and 1% powdered milk, and were incubated with a 1:50 dilution of Texas red-conjugated goat anti-rabbit antibodies (Southern Biotechnologies, Birmingham, AL) for 2 hr at 37°C. The slides were then mounted with an antifade reagent in glycerol buffer (Slowfade; Molecular Probes) and viewed with a Nikon fluorescence microscope (Japan) using a confocal laser scanning unit (Molecular Dynamics model 2010). Excitation was at 488 nm and emission was at 515–545 nm for FITC. For Texas red, excitation was at 568 nm and emission was at >590 nm. Images were processed as anaglyphs on a SGI computer system (Molecular Dynamics). Negative controls for nonspecific binding, incubated with secondary antibody only, were processed and found to reveal no signal.

RESULTS

***Atm*-Deficient Mice Show Evidence of Oxidative Damage to Proteins and Lipids.** To study the role of oxidative stress *in vivo* in organs affected by loss of ATM function, tissues from *Atm*-deficient mice were isolated, and markers of oxidative damage to proteins and lipids were measured. Proteins are targets of both reactive-oxygen and reactive-nitrogen species, generating a large number of products (7). We measured nitric oxide-mediated oxidative damage to proteins, assaying for 3-nitrotyrosine (9), and found that *Atm*-deficient mice have elevated nitrotyrosine in the brain (Fig. 1*A*). Nitrotyrosine/tyrosine values in control brains were clustered near their mean of 1.1 μmol/mol of tyrosine, whereas three of the four *Atm*-deficient brains had values over 2 ($P < 0.048$). In contrast, analysis of livers from these animals showed no difference in the ratio of nitrotyrosine to tyrosine (data not shown). This observation indicates that the brain, but not the liver, shows evidence of oxidative damage in the absence of ATM.

Oxidized protein-bound products can also contain carbonyl groups. The presence of carbonyl groups in oxidized proteins has become a widely accepted measure of oxidative damage (7). To test whether this form of oxidized product was present, protein carbonyl levels were measured by the quantitative HPLC method on tissue homogenates from three animals of each genotype. No significant difference between *Atm*-deficient and wild-type littermate mice was detected in any tissue examined, namely cerebellum, cerebral cortex, liver, testis, and thymus (data not shown). These findings were confirmed by using Western blotting to detect any elevations in specific proteins that might be missed by taking the average carbonyl level in the homogenates (10). Western blotting similarly revealed no differences (data not shown). Thus, there is no global increase in oxidative modification of proteins present in higher amount, but the available assays are not sensitive enough to detect increases in proteins present in lower concentration.

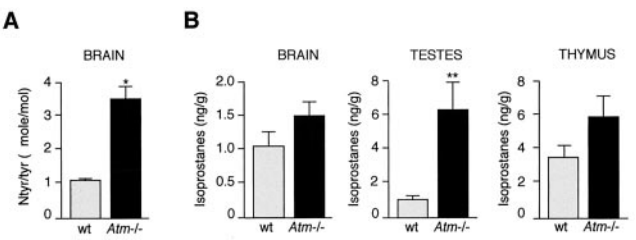

FIG. 1. Proteins and lipids are covalently modified in the absence of ATM. (*A*) Mean ratio of nitrotyrosine to tyrosine in whole brain from 3-month-old wild-type (wt) animals (gray bar, $n = 5$ animals) and *Atm*-deficient (*Atm*−/−) animals (black bar, n = four animals). (*B*) Mean level of F_2-isoprostanes from brain, testes, and thymus in wild-type (gray bars) and age-matched *Atm*-deficient mice (black bars). *, Significance with $P < 0.048$; **, significance with $P < 0.01$. Error bars represent ±SEM. Statistical analyses were performed with Fisher's exact test.

To determine whether lipids were damaged by oxidative stress, we quantitated levels of F_2-isoprostanes, which are chemically stable peroxidation products of arachidonic acid. It has been shown that F_2-isoprostanes are specific markers of oxidative stress *in vivo*, generally superior to other assays for lipid peroxidation as indicators of oxidant stress (13, 14). As shown in Fig. 1*B*, F_2-isoprostanes were elevated in the testes of *Atm*-deficient mice ($n = 6$ wild-type and 7 *Atm*-deficient mice, 1.46 ± 0.35 vs. 6.23 ± 2.58 ng/g; $P < 0.01$). In thymus and brain, there was a trend toward elevation but it did not reach statistical significance. The values for thymus were 3.52 ± 1.45 ng/g in wild-type and 5.46 ± 3.45 ng/g in the *Atm*-deficient mice ($n = 10$ animals in each group; $P < 0.13$). Brain showed levels of 1.16 ± 0.45 vs. 1.43 ± 0.49 ng/g, respectively ($n = 3$ animals in each group; $P < 0.48$).

HO-1 Is Specifically Elevated in the Purkinje Cells of *Atm*-Deficient Mice. The analyses of modified macromolecules established that loss of ATM leads to increased oxidative damage in targeted tissues. We then assessed whether cells were sensing and responding to the oxidative stress. We thus characterized the content and activity of the HO isozymes because changes in HO are a generalized response to oxidative stress from multiple stimuli (15). Two different genes encode proteins with HO activity, HO-1 and HO-2. HO-1 is the inducible form, whereas HO-2 is constitutively expressed and is especially abundant in neurons. HO is the rate-limiting step in the metabolism of heme. HO converts heme, an oxidant, to biliverdin, with release of iron and carbon monoxide. Biliverdin is then reduced to the antioxidant bilirubin by biliverdin reductase. HO is postulated to play a key role as an antioxidant defense enzyme (16). Further, HO prevents neuronal damage and death in response to various oxidative and ischemic insults, presumably through removal of oxidants and production of antioxidant (12, 17, 18).

We focused on the brain, the organ most severely affected in A-T patients. We found that mRNA and protein levels of both HO-1 and HO-2 were increased in the cerebral cortex and cerebellum of 3-month-old *Atm*-deficient mice (Fig. 2*A* and data not shown). The expression of HO-1 mRNA was increased by ≈28% in the cerebellum of *Atm*-deficient mice and by 14% in the cortex (average of two separate determinations). HO-2 increased by 23% in the cerebellum of the *Atm*-deficient mouse, and by 12% in cortex. These modest changes in mRNA prompted us to determine the specific activity of HO in brain, because it is the change in activity that carries functional significance (Fig. 2*B*). Total HO activity in the cortex did not differ between the wild-type and *Atm*-deficient mice. However, the cerebellum of *Atm*-deficient mice had a remarkable 600% increase in HO activity.

Immunohistochemical staining was then employed to determine which of the HO isozymes was elevated and whether the increase was global or localized. As shown in Fig. 3, HO-1 was increased in the Purkinje cell layer of the *Atm*-deficient mouse, whereas staining in the granular cell layer was similar in *Atm*-deficient and wild-type mice. The increase of HO-1 in Purkinje cells was present in both the cell soma and dendrites.

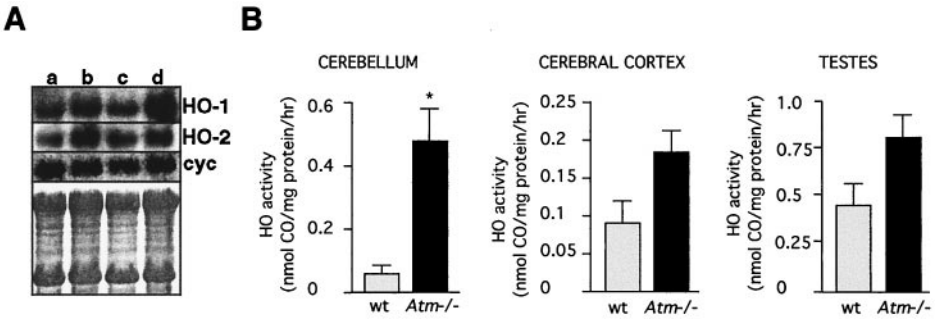

FIG. 2. Increased expression and activity of HO in brains from *Atm*-deficient mice. (*A*) Representative Northern blot of 10 μg of total RNA isolated from 3-month-old male littermates as follows: wild-type cerebral cortex (lane a); *Atm*-deficient cerebral cortex (lane b); wild-type cerebellum (lane c); and *Atm*-deficient cerebellum (lane d). cyc, Cyclophilin control. The bottom box is the methylene blue-stained blot for assessing RNA loading. (*B*) Total HO activity in the cerebellum, cerebral cortex, and testes of *Atm*-deficient (gray bars) and wild-type mice (black bars). Each bar represents the mean ± SEM. Statistical significance of differences between and within groups was assessed with the unpaired *t* test with the Scheffe correction for multiple comparisons. *, Significance with $P < 0.05$. Three animals of each genotype at 3 months of age were used for the HO activity determinations. The specific activity in wild-type cerebellum was 77 pmol of CO per mg of protein per hr; in *Atm*-deficient animals it was 458 pmol of CO per mg per hr ($P < 0.05$). The values for wild-type and *Atm*-deficient cortex and testes were not statistically significantly different.

In the cortex, no difference in HO-1 staining between wild-type and mutant was detected (data not shown). HO-2 staining was increased in both cortex and cerebellum of the *Atm*-deficient brain. The increase was seen throughout the tissue, but most notably around blood vessels in the cerebral cortex (Fig. 3 *C* and *D* and data not shown for the cerebellum).

Taken together, these analyses indicate that the increase in HO activity in the cerebellum is likely caused by an increase of HO-1 in Purkinje cells. However, Dore and colleagues (19) recently demonstrated that HO-2 is a substrate of protein kinase C and that phosphorylation increases the catalytic activity of this isozyme. It is therefore possible that a portion of the increased HO activity in the *Atm*-deficient cerebellum is a result of activation of HO-2 by phosphorylation.

DISCUSSION

Our experimental results establish that tissues from *Atm*-deficient mice are under oxidative stress and suffer oxidative damage. We and others have identified defects in molecular pathways that lead to abnormalities in the response of cells to ionizing radiation, meiosis, and T cell development where DNA double-strand breaks occur (1, 3–5, 20–23). In addition, several reports have implicated ATM as a serine protein kinase that phosphorylates p53 and chk2, leading to cell cycle arrest after ionizing radiation (24–27). Why would defects in these pathways result in oxidative stress, especially in the adult brain? The majority of cells in the central nervous system are postmitotic and there is no evidence of DNA recombination or significant DNA double-strand breaks in the central nervous system in the absence of ionizing radiation. We infer that ATM also functions to protect biomolecules other than DNA from oxidative damage. Studies from many investigators have established that lipids and proteins are also targets of oxidative damage in cells, and considerable evidence suggests that oxidation of these macromolecules is important in the pathophysiology and progression of a variety of diseases (7).

How ATM, possibly acting as a PI-3 kinase, alters components of oxidative defense mechanisms is a matter of speculation. However, studies of a different PI-3 kinase in *Caenorhabditis elegans* provide an example in which mutation of the gene affects oxidative defense and causes a profound change in the process of aging (28, 29). These investigators reported that mutations in *age-1* led to increased lifespan in the worms carrying the alteration. One hypothesis of aging is that it is a consequence of the accumulation of oxidative damage to cells, an inevitable consequence of leakage of reactive species during normal metabolism. This led the discoverers of *age-1* to assess the oxidative defenses of their mutant, and they found a substantial increase in antioxidant activities, especially of catalase. Subsequently *age-1* was shown to encode not an antioxidant enzyme, but a PI-3 kinase. Recently, the investigators showed that *C. elegans* has a gene encoding a cytosolic catalase, distinct from the well-known peroxisomal catalase. *Age-1* causes increased expression and synthesis of this cytosolic catalase, and overexpression by transfection also confers increased longevity. Thus, mutations in a PI-3 kinase, *age-1*, lead to increases in the antioxidant defense system. In the case of *Atm*, mutations lead to decreased resistance to oxidative stress.

Is the observed oxidative stress secondary to an ongoing degenerative process rather than being a cause of the degeneration? This could be the case in the testes, where significant degeneration of abnormal germ cells occurs (23). However, this oxidative stress caused by degeneration appears unlikely in the thymus or brain. The *Atm*-deficient mice show evidence of early neurobehavioral dysfunction that precedes frank neurodegeneration. Thus, we found no evidence of increased cell death or of inflammation in the brains of our mice by using terminal deoxynucleotidyltransferase-mediated UTP end labeling (TUNEL) staining, immunohistochemical markers for microglia, and electron microscopic histology (C.B., unpublished results). Similarly, *Atm*-deficient thymus does not exhibit increased apoptosis (1, 20).

Ataxia, a hallmark of A-T, is an early clinical finding in patients and is a consequence of Purkinje cell dysfunction. The finding of markedly increased HO activity in the *Atm*-deficient mouse is therefore of particular interest. We previously established that alterations in HO activity affect resistance of cells to oxidative damage. Whether resistance is increased or decreased depends on the quantitative level of activity, following what has been termed a hormetic response (30). That is, cells with decreased HO activity are more susceptible to oxidative damage. Modest increases in HO-1 activity above basal levels will increase resistance to oxidative stress, but further increases render the cells more susceptible to oxidative damage (31). Given this "U-shaped" or hormetic response, one cannot predict the effect of inhibiting the 6-fold increase in HO activity observed in the cerebellum of the *Atm*-deficient mouse, but the experiment is of obvious interest.

The mechanism by which high levels of HO-1 cause cellular damage is not proven, but it has been proposed that it results from increased availability of pro-oxidant iron released from heme (31). Recent studies of HO-2 knockout mice documented that iron deposition correlated with over-expression of HO-1 in the lung parenchyma (12), and deletion of HO-1 leads

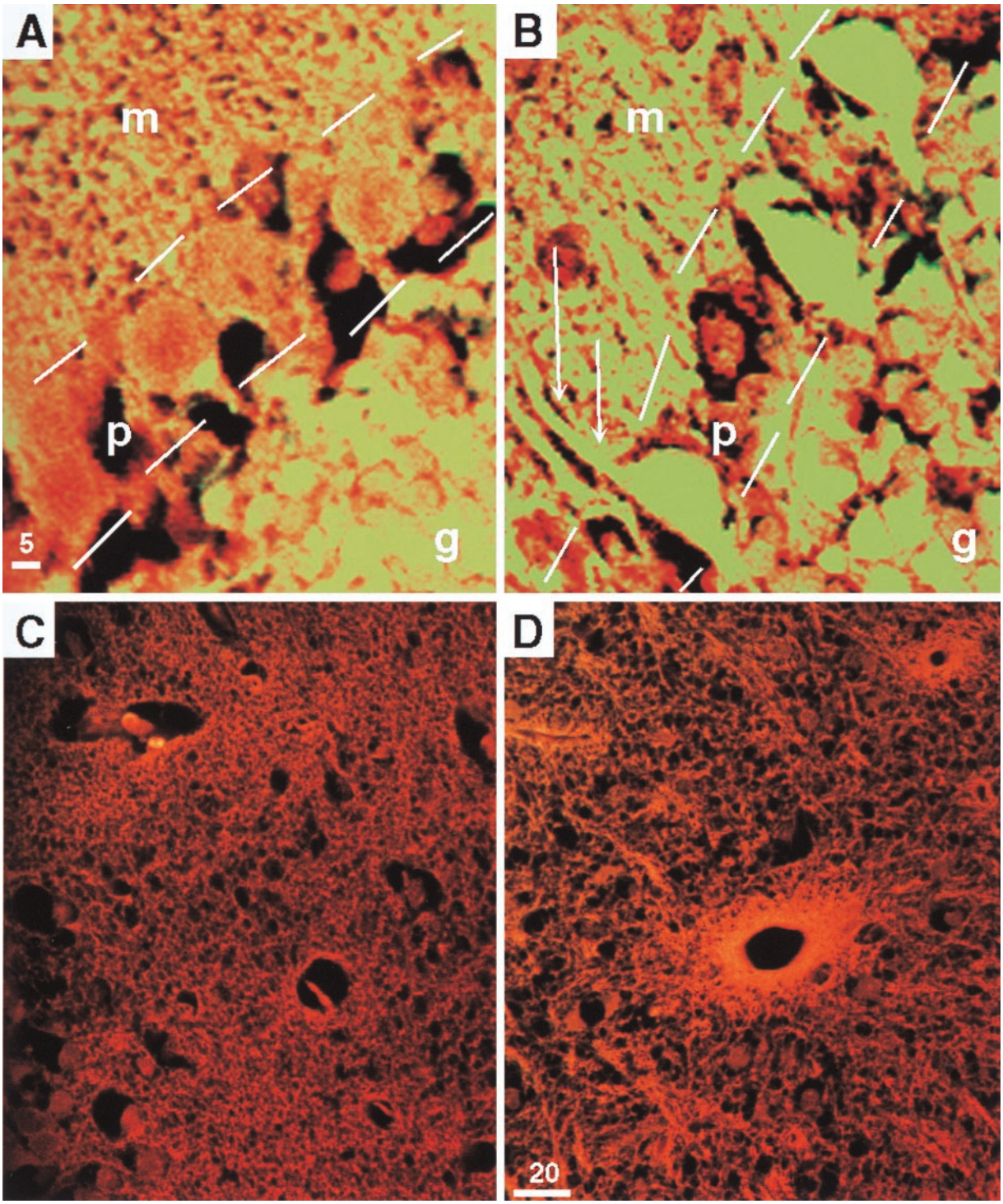

FIG. 3. Purkinje cells and cells surrounding blood vessels show increased levels of HO protein in the absence of ATM. The yellow fluorescent signal shown in *A* and *B* is from anti-HO-1 staining in a wild-type (*A*) and *Atm*-deficient (*B*) mouse cerebellum at high magnification (×100) to show the significant increase in staining in the Purkinje cell layer. m Indicates the molecular layer, p and outline indicate the Purkinje cell layer, and g indicates the granular cell layer. Note the intense signal in the Purkinje cell soma of the *Atm*-deficient brain in *B*. The increased staining in the molecular layer is likely caused by HO in the dendritic arbors, as the spines are well demarcated by the intense staining (double arrows). The granular cell layer (g) staining is similar in the wild-type and *Atm*-deficient animals. *C* (wild-type) and *D* (*Atm*-deficient) show the increase in bright orange signal from anti-HO-2, which is prominent in cells surrounding the vasculature of the cerebral cortex in the *Atm*-deficient mouse (*D*). (×40.)

to similar pathological sequelae with iron deposition in other tissues without clear changes in HO-2 activity (17). Also, in one recently described HO-1-deficient individual, iron deposition in the vasculature also increased (32). Thus, an overly robust increase in HO in response to oxidative stress may increase tissue damage through iron-catalyzed oxidation.

We also observed that HO is elevated in the cells surrounding the vasculature. Thus, the vasculature and surrounding tissues may also be targets of oxidative damage. Although telangiectasias (abnormal blood vessels) have been reported in A-T patients, these have generally been confined to the skin and cornea. The finding of elevated HO-2 suggests that

endothelial cell dysfunction may contribute to the pathology of A-T.

Atm-deficient animals have elevated levels of oxidized macromolecules and of heme oxygenase in tissues phenotypically affected by the mutation, particularly the cerebellum. A-T should be added to the growing list of neurodegenerative disorders characterized by disorders in oxidative processes (6), and the animal model can now be exploited to assess the efficacy of therapies aimed at minimizing oxidative damage caused by the disease.

We acknowledge Denise Larson for technical support, Amber Pope for assistance with immunohistochemistry, Nancy Wehr for performing the protein carbonyl assays, Daniel G. Pankratz for assistance with RNA analysis, Yi-Hao Weng for technical assistance in performing the immunohistochemistry and HO activity measurements, and David R. Schubert for critical review of the manuscript. This work was supported by National Institutes of Health Grants HL58782 to P.A.D. and GM42056, DK48831, and GM15431 to L.J.R.; J.D.M. is supported by a Burroughs Wellcome Fund Clinical Scientist Award in Translational Research. C.B. is supported by The Frederick B. Rentschler Developmental Chair and a grant from the Ataxia–Telangiectasia Children's Fund.

1. Barlow, C., Hirotsune, S., Paylor, R., Liyanage, M., Eckhaus, M., Collins, F., Shiloh, Y., Crawley, J., Ried, T., Tagle, D. & Wynshaw-Boris, A. (1996) *Cell* **86,** 159–171.
2. Savitsky, K., Bar-Shira, A., Gilad, S., Rotman, G., Ziv, Y., Vanagaite, L., Tagle, D. A., Smith, S., Uziel, T., Sfez, S., *et al.* (1995) *Science* **268,** 1749–1753.
3. Xu, Y., Ashley, T., Brainerd, E., Bronson, R., Meyn, M. & Baltimore, D. (1996) *Genes Dev.* **10,** 2411–2422.
4. Rotman, G. & Shiloh, Y. (1998) *Hum. Mol. Genet.* **7,** 1555–1563.
5. Brown, K., Barlow, C. & Wynshaw-Boris, A. (1999) *Am. J. Hum. Genet.* **64,** 46–50.
6. Coyle, J. T. & Puttfarcken, P. (1993) *Science* **262,** 689–695.
7. Stadtman, E. R. & Berlett, B. S. (1997) *Chem. Res. Toxicol.* **10,** 485–494.
8. Pratico, D., Lee, V. M.-Y., Trojanowski, J. Q., Rokach, J. & FitzGerald, G. A. (1998) *FASEB J.* **12,** 1777–1783.
9. Shigenaga, M. K., Lee, H. H., Blount, B. C., Christen, S., Shigeno, E. T., Yip, H. & Ames, B. N. (1997) *Proc. Natl. Acad. Sci. USA* **94,** 3211–3216.
10. Levine, R. L., Williams, J. A., Stadtman, E. R. & Shacter, E. (1994) *Methods Enzymol.* **233,** 346–357.
11. Morrow, J. D., Harris, T. M. & Roberts, L. J., 2nd (1990) *Anal. Biochem.* **184,** 1–10.
12. Dennery, P., Spitz, D., Yang, G., Tatarov, A., Lee, C., Shegog, M. & Poss, K. (1998) *J. Clin. Invest.* **101,** 1001–1011.
13. Salahudeen, A., Badr, K., Morrow, J. & Roberts, J., 2nd (1995) *J. Am. Soc. Nephrol.* **6,** 1300–1303.
14. Liu, T., Stern, A. & Morrow, J. (1998) *J. Biomed. Sci.* **5,** 415–420.
15. Applegate, L., Luscher, P. & Tyrrell, R. (1991) *Cancer Res.* **51,** 974–978.
16. Dennery, P., Sridhar, K., Lee, C., Wong, H., Shokoohi, V., Rodgers, P. & Spitz, D. R. (1997) *J. Biol. Chem.* **272,** 14937–14942.
17. Poss, K. & Tonegawa, S. (1997) *Proc Natl. Acad. Sci. USA* **94,** 10919–10924.
18. Takizawa, S., Hirabayashi, H., Matsushima, K., Tokuoka, K. & Shinohara, Y. (1998) *J. Cereb. Blood Flow Metab.* **18,** 559–569.
19. Dore, S., Takahashi, M., Ferris, C. D., Hester, L. D., Guastella, D. & Snyder, S. H. (1999) *Proc. Natl. Acad. Sci. USA* **96,** 2445–2450.
20. Barlow, C., Brown, K., Deng, C. X., Tagle, D. & Wynshaw-Boris, A. (1997) *Nat. Genet.* **17,** 453–456.
21. Barlow, C., Liyanage, M., Moens, P., Deng, C. X., Ried, T. & Wynshaw-Boris, A. (1997) *Nat. Genet.* **17,** 462–466.
22. Westphal, C. H., Rowan, S., Schmaltz, C., Elson, A., Fisher, D. E. & Leder, P. (1997) *Nat. Genet.* **16,** 397–401.
23. Barlow, C., Liyanage, M., Moens, P., Nagashima, K., Brown, K., Rottinghaus, S., Jackson, S., Tagle, D., Ried, T. & Wynshaw-Boris, A. (1998) *Development (Cambridge, U.K.)* **125,** 4007–4017.
24. Canman, C., Lim, D., Cimprich, K., Taya, Y., Tamai, K., Sakaguchi, K., Appella, E., Kastan, M. & Siliciano, J. (1998) *Science* **281,** 1677–1679.
25. Banin, S., Moyal, L., Shieh, S., Taya, Y., Anderson, C., Chessa, L., Smorodinsky, N., Prives, C., Reiss, Y., Shiloh, Y. & Ziv, Y. (1998) *Science* **281,** 1674–1677.
26. Khanna, K., Keating, K., Kozlov, S., Scott, S., Gatei, M., Hobson, K., Taya, Y., Gabrielli, B., Chan, D., Lees-Miller, S. & Lavin, M. (1998) *Nat. Genet.* **20,** 398–400.
27. Matsuoka, S., Huang, M. & Elledge, S. (1998) *Science* **282,** 1893–1897.
28. Morris, J. Z., Tissenbaum, H. A. & Ruvkun, G. (1996) *Nature (London)* **382,** 536–539.
29. Taub, J., Lau, J. F., Ma, C., Hahn, J. H., Hoque, R., Rothblatt, J. & Chalfie, M. (1999) *Nature (London)* **399,** 162–166.
30. Furst, A. (1987) *Health Phys.* **52,** 527–530.
31. Suttner, D. M. & Dennery, P. A. (1999) *FASEB J.,* in press.
32. Yachie, A., Niida, Y., Wada, T., Igarashi, N., Kaneda, H., Toma, T., Ohta, K., Kasahara, Y. & Koizumi, S. (1999) *J. Clin. Invest.* **103,** 129–135.